Finite-Volume Effects to the HVP in QCD with C* Boundary Conditions

Paola Tavella (ETH Zürich)
RC* collaboration

The 43rd International Symposium on Lattice Field Theory

28 July 2026

Motivation

Finite-volume effects in lattice computations

Lattice simulations are performed in finite volume (FV) $\to$ IR cutoff

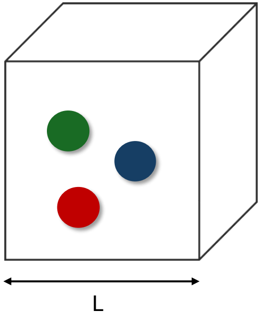

- Momenta are quantized

$$\vec{p} \in \mathbb{R}^3 \;\to\; \vec{p}_n \in \Pi$$

- Virtual particle propagation is modified

$$\int \frac{d^4\vec{p}}{(2\pi)^4} f(p) \;\to\; \frac{1}{L^3} \int \frac{dp_0}{(2\pi)} \sum_{\vec{p}_n \in \Pi} f(p_0, \vec{p}_n)$$

- Finite-T effects usually subleading as $T \sim 2L$

Finite-volume effects in lattice computations

Lattice simulations are performed in finite volume (FV) $\rightarrow$ IR cutoff

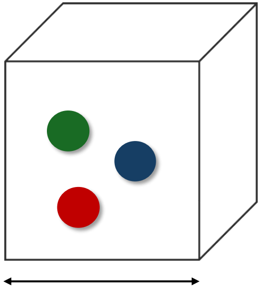

- Momenta are quantized

$$\vec{p} \in \mathbb{R}^3 \;\rightarrow\; \vec{p}_n \in \Pi$$

- Virtual particle propagation is modified

$$\int \frac{d^4\vec{p}}{(2\pi)^4} f(p) \;\rightarrow\; \frac{1}{L^3} \int \frac{dp_0}{(2\pi)} \sum_{\vec{p}_n \in \Pi} f(p_0, \vec{p}_n)$$

- Finite-T effects usually subleading as $T \sim 2L$

QCD (Lüscher, 1986)
mass gap $\Longrightarrow$ $\Delta_L M^{\text{had}} \sim e^{-m_{\text{gap}} L}$

QED (e.g., Hayakawa & Uno, 2008)
massless field $\Longrightarrow$ $\Delta_L M^{\text{had}} \sim \frac{1}{L^p}$

Finite-volume effects with C* boundary conditions

In the RC* collaboration we use C* boundary conditions in the spatial directions:
(Kronfeld & Wiese, 1991; Lucini et al., 2015)

$$A_\mu(x + L_k \hat{k}) = -A_\mu(x) \qquad U_\mu(x + L_k \hat{k}) = U_\mu^*(x)$$

$$\psi(x + L_k \hat{k}) = C^{-1} \bar{\psi}(x)^\top \qquad \bar{\psi}(x + L_k \hat{k}) = -\psi^\top(x)\, C$$

- Prescription to remove the zero-momentum mode of A_μ in FV QCD+QED calculations (see previous works from RC* collaboration)
- Imposed for all fields $\implies$ different FV effects in QCD compared to pbc

Finite-volume effects with C* boundary conditions

In the RC* collaboration we use C* boundary conditions in the spatial directions:
(Kronfeld & Wiese, 1991; Lucini et al., 2015)

$$A_\mu(x + L_k\hat{k}) = -A_\mu(x) \qquad U_\mu(x + L_k\hat{k}) = U^*_\mu(x)$$

$$\psi(x + L_k\hat{k}) = C^{-1}\bar{\psi}(x)^\top \qquad \bar{\psi}(x + L_k\hat{k}) = -\psi^\top(x)\, C$$

- Prescription to remove the zero-momentum mode of A_μ in FV QCD+QED calculations (see previous works from RC* collaboration)
- Imposed for all fields $\Longrightarrow$ different FV effects in QCD compared to pbc

This talk: FV-dependence of the muon's HVP in QCD with C* boundary conditions

1. First look at the lattice results for different physical L
2. Ongoing work towards a theoretical expression for FV effects in our setup

Numerical computation

The isovector window contribution to the muon's HVP

In time-momentum representation (Bernecker & Meyer, 2011):

$$a_\mu^{33,\mathrm{IW}} = \int_0^\infty \mathrm{d}t\, G^{33}(t)\tilde{K}(t; m_\mu) w_\mathrm{I}(t)$$

- $G^{33}(t)$ correlator of two isovector currents $V_\mu^3 = \frac{1}{2}(\overline{\psi}_\mathrm{u}\gamma_\mu\psi_\mathrm{u} - \overline{\psi}_\mathrm{d}\gamma_\mu\psi_\mathrm{d})$
- point-split local discretization of the correlator
- $w_\mathrm{I}(t)$ intermediate window kernel (Blum et al., 2018)
- Disconnected-free contribution due to isospin symmetry

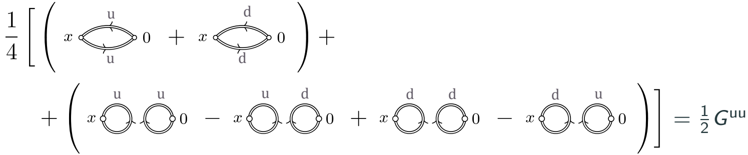

Setup and computation of $a_\mu^{33,\mathrm{IW}}$

RC* gauge ensembles:

- $N_f = 3 + 1$ Wilson fermions
- Unphysical light quark masses

Ensemble	L [fm]	m_π [MeV]	$m_\pi L$
A400	1.73	398.5(4.7)	~ 3.5
AB400	1.93	407.5(4.2)	~ 4.0
B400	2.59	401.9(1.4)	~ 5.2
D400	3.44	402.4(1.5)	~ 7

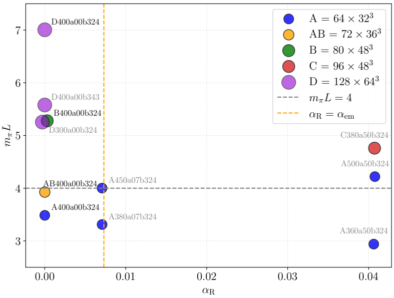

Setup and computation of $a_\mu^{33,\mathrm{IW}}$

RC* gauge ensembles:

- $N_f = 3+1$ Wilson fermions
- Unphysical light quark masses

Ensemble	L [fm]	m_π [MeV]	$m_\pi L$
A400	1.73	398.5(4.7)	~ 3.5
AB400	1.93	407.5(4.2)	~ 4.0
B400	2.59	401.9(1.4)	~ 5.2
D400	3.44	402.4(1.5)	~ 7

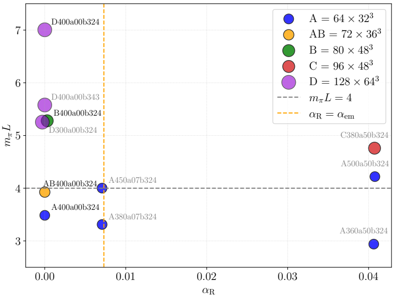

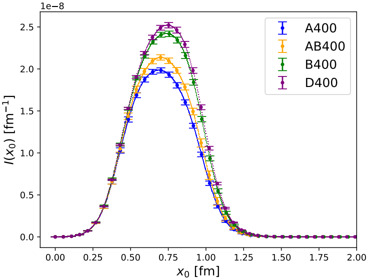

Results:

Ensemble	$N_c \times N_s$	$a_\mu^{33,\mathrm{IW}} \times 10^{10}$
A400	1000 $\times$ 4	109.0(7)
AB400*	250 $\times$ 12	117.0(9)
B400	500 $\times$ 8	134.6(8)
D400	470 $\times$ 8	140.0(8)

* Lower statistics, RW factor missing

Observed FV effects of $a_\mu^{33,\mathrm{IW}}$

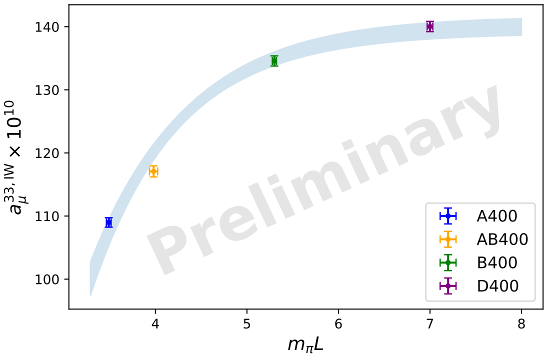

- Taking D400 as our reference box:

$$a_\mu^{33,\mathrm{IW}}(\mathrm{A400}) - a_\mu^{33,\mathrm{IW}}(\mathrm{D400}) = -31(1) \times 10^{-10}$$
$$a_\mu^{33,\mathrm{IW}}(\mathrm{AB400}) - a_\mu^{33,\mathrm{IW}}(\mathrm{D400}) = -23(1) \times 10^{-10}$$
$$a_\mu^{33,\mathrm{IW}}(\mathrm{B400}) - a_\mu^{33,\mathrm{IW}}(\mathrm{D400}) = -5.5(1.1) \times 10^{-10}$$

Comparison with periodic-boundary FV estimates

Dominant finite-L effect from Hansen–Patella method (Hansen & Patella, 2020)

$$\Delta a_s^{pole}(L) = -\int_0^\infty dx_0 \tilde{K}(x_0) \sum_{\vec{n}\neq 0} \int \frac{dp_3}{2\pi} \frac{e^{-nL\sqrt{m_\pi^2+p_3^2}}}{6\pi nL} \,\mathrm{Re} \int \frac{dk_3}{2\pi} e^{ik_3 x_0} \frac{(4m_\pi^2 + k_3^2) F(-k_3^2)^2}{k_3^2 + 2k_3 p_3 - i\epsilon}$$

- $F(q^2) = 1 - q^2/M^2$, $M^2(m_\pi^2) = 0.517(23)\mathrm{GeV}^2 + 0.647(30) m_\pi^2$ (Brömmel et al., 2006)

Comparison with periodic-boundary FV estimates

Dominant finite-L effect from Hansen–Patella method (Hansen & Patella, 2020)

$$\Delta a_s^{pole}(L) = -\int_0^\infty dx_0 \tilde{K}(x_0) \sum_{\vec{n}\neq 0} \int \frac{dp_3}{2\pi} \frac{e^{-nL\sqrt{m_\pi^2+p_3^2}}}{6\pi nL} \mathrm{Re} \int \frac{dk_3}{2\pi} e^{ik_3x_0} \frac{(4m_\pi^2+k_3^2)F(-k_3^2)^2}{k_3^2+2k_3p_3-i\epsilon}$$

- $F(q^2) = 1 - q^2/M^2,\ M^2(m_\pi^2) = 0.517(23)\mathrm{GeV}^2 + 0.647(30)m_\pi^2$ (Brömmel et al., 2006)

Expected FV effects with pbc vs C* data:

- Estimates for $a_\mu^{33,\mathrm{IW}}(\infty) - a_\mu^{33,\mathrm{IW}}(L)$ at SU(3) point for three values of m_π

$m_\pi L$	m_π^{phys}	$2m_\pi^{\mathrm{phys}}$	$3m_\pi^{\mathrm{phys}}$	From C* data
3.5	$1.8\cdot10^{-10}$	$6.6\cdot10^{-10}$	$1.3\cdot10^{-9}$	$3.1(1)\cdot10^{-9}$
4.0	$9.5\cdot10^{-11}$	$3.6\cdot10^{-10}$	$6.9\cdot10^{-10}$	$2.3(1)\cdot10^{-9}$
5.2	$2.10\cdot10^{-11}$	$8.7\cdot10^{-11}$	$1.7\cdot10^{-10}$	$5(1)\cdot10^{-10}$
6.0	$8.40\cdot10^{-12}$	$3.5\cdot10^{-11}$	$7.0\cdot10^{-11}$	–
7.0	$2.70\cdot10^{-12}$	$1.2\cdot10^{-11}$	$2.4\cdot10^{-11}$	–

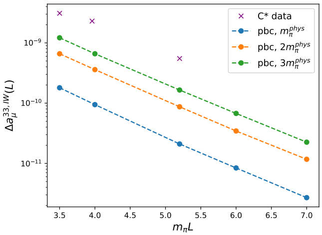

Analytical study of FV effects

Generalizing Hansen–Patella method to C* boundaries

Leading-order FV effects studied using a Hamiltonian representation of the correlator in a box with $L_\rho = (L_\perp, L_\perp, L_\perp, L)$ (Hansen & Patella, 2019)

$$G_{L_\rho}(x_0) = -\frac{1}{3}\int_0^{L_\perp} d^2\vec{x}_\perp \int_0^{L} dx_3 \left\langle T_3\{j_\mu(x_0,\vec{x}_\perp,x_3) j_\mu(0,\vec{0},L/2)\}\right\rangle_{L_\rho} =$$

$$= -\frac{1}{3}\int_0^{L_\perp} d^2\vec{x}_\perp \int_0^{L} dx_3 \frac{\mathrm{tr}\left[\mathcal{B}e^{-LH} T_3\{j_\mu(x_0,\vec{x}_\perp,x_3) j_\mu(0,\vec{0},L/2)\}\right]}{\mathrm{tr}[\mathcal{B}e^{-LH}]}$$

- x_3 is the direction of quantization
- H has a discrete spectrum in $L_\perp^3$
- $\mathcal{B}$ implements the boundaries on states $\Longrightarrow$ $(-1)^F$ for pbc, $U_{\mathcal{C}}$ for C* bc

Steps of the calculation

$$G_{L_\rho}(x_0) = -\frac{1}{3}\int_0^{L_\perp} d^2\vec{x}_\perp \int_0^{L} dx_3 \, \frac{\mathrm{tr}\left[\mathcal{B} e^{-LH} T_3\{j_\mu(x_0,\vec{x}_\perp,x_3) j_\mu(0,\vec{0},L/2)\}\right]}{\mathrm{tr}\left[\mathcal{B} e^{-LH}\right]}$$

1. Insert complete basis of eigenstates of $H, p, U_{\mathcal{C}}$: $|n\rangle$

Steps of the calculation

$$G_{L_\rho}(x_0) = -\frac{1}{3}\int_0^{L_\perp} d^2\vec{x}_\perp \int_0^L dx_3 \frac{\mathrm{tr}\left[\mathcal{B}e^{-LH}T_3\{j_\mu(x_0,\vec{x}_\perp,x_3)j_\mu(0,\vec{0},L/2)\}\right]}{\mathrm{tr}\left[\mathcal{B}e^{-LH}\right]}$$

1. Insert complete basis of eigenstates of $H, p, U_{\mathcal{C}}$: $|n\rangle$
2. Integration over x_3

$$G_{L_\rho}(x_0) = -\frac{1}{3}\int_0^{L_\perp} d^2\vec{x}_\perp \sum_{n,n'} \frac{M_{nn'}(x_0,\vec{x}_\perp)}{Z}\chi_n \begin{cases} 2\frac{e^{-LE_n}-e^{-L/2(E_n+E_n')}}{E_{n'}-E_n}, & E_n \neq E_{n'} \\ Le^{-LE_n}, & E_n = E_{n'} \end{cases}$$

- $M_{nn'}(x_0,\vec{x}_\perp) = \langle n|j_\mu(x_0,\vec{x}_\perp)|n'\rangle\langle n'|j_\mu(0)|n\rangle$
- $\chi_n = 1$, $Z = \sum_n e^{-LE_n}$, $\chi_n = \eta_n^c$,$Z = \sum_n \eta_n^c e^{-LE_n}$ $\rightarrow$ **selection rule for** $|n\rangle, |n'\rangle$

Steps of the calculation

$$G_{L_\rho}(x_0) = -\frac{1}{3}\int_0^{L_\perp} d^2\vec{x}_\perp \int_0^L dx_3 \frac{\mathrm{tr}\left[\mathcal{B}e^{-LH}T_3\{j_\mu(x_0,\vec{x}_\perp,x_3)j_\mu(0,\vec{0},L/2)\}\right]}{\mathrm{tr}\left[\mathcal{B}e^{-LH}\right]}$$

1. Insert complete basis of eigenstates of $H, p, U_{\mathcal{C}}$: $|n\rangle$
2. Integration over x_3

$$G_{L_\rho}(x_0) = -\frac{1}{3}\int_0^{L_\perp} d^2\vec{x}_\perp \sum_{n,n'} \frac{M_{nn'}(x_0,\vec{x}_\perp)}{Z}\chi_n \begin{cases} 2\,\dfrac{\overset{①}{e^{-LE_n}} - \overset{②}{e^{-L/2(E_n+E_n')}}}{E_{n'}-E_n}, & E_n \neq E_{n'} \\ \underset{③}{Le^{-LE_n}}, & E_n = E_{n'} \end{cases}$$

   - $M_{nn'}(x_0,\vec{x}_\perp) = \langle n|j_\mu(x_0,\vec{x}_\perp)|n'\rangle\langle n'|j_\mu(0)|n\rangle$
   - $\chi_n = 1$, $Z = \sum_n e^{-LE_n}$, $\chi_n = \eta_n^c$,$Z = \sum_n \eta_n^c e^{-LE_n}$ $\rightarrow$ **selection rule for** $|n\rangle, |n'\rangle$

3. Expand for large L and isolate $\Delta G(x_0|L_\perp, L) = G(x_0|L_\perp, L) - G(x_0|L_\perp,\infty)$

$$\text{pbc}: ① + ③, \qquad \text{C}^\star: ① + ②$$

Steps of the calculation

$$G_{L_\rho}(x_0) = -\frac{1}{3}\int_0^{L_\perp} d^2\vec{x}_\perp \int_0^L dx_3 \frac{\mathrm{tr}\left[\mathcal{B}e^{-LH}T_3\{j_\mu(x_0,\vec{x}_\perp,x_3)j_\mu(0,\vec{0},L/2)\}\right]}{\mathrm{tr}\left[\mathcal{B}e^{-LH}\right]}$$

1. Insert complete basis of eigenstates of $H, p, U_{\mathcal{C}}$: $|n\rangle$
2. Integration over x_3

$$G_{L_\rho}(x_0) = -\frac{1}{3}\int_0^{L_\perp} d^2\vec{x}_\perp \sum_{n,n'} \frac{M_{nn'}(x_0,\vec{x}_\perp)}{Z}\chi_n \begin{cases} 2\,\dfrac{\overset{①}{e^{-LE_n}} - \overset{②}{e^{-L/2(E_n+E_n')}}}{E_{n'}-E_n}, & E_n \neq E_{n'} \\ \underset{③}{Le^{-LE_n}}, & E_n = E_{n'} \end{cases}$$

- $M_{nn'}(x_0,\vec{x}_\perp) = \langle n|j_\mu(x_0,\vec{x}_\perp)|n'\rangle\langle n'|j_\mu(0)|n\rangle$
- $\chi_n = 1$, $Z = \sum_n e^{-LE_n}$, $\chi_n = \eta_n^c$,$Z = \sum_n \eta_n^c e^{-LE_n}$ $\rightarrow$ **selection rule for** $|n\rangle, |n'\rangle$

3. Expand for large L and isolate $\Delta G(x_0|L_\perp, L) = G(x_0|L_\perp, L) - G(x_0|L_\perp, \infty)$

$$\mathrm{pbc}: ① + ③, \qquad \mathrm{C}^\star: ① + ②$$

4. Take the limit for $L_\perp \rightarrow \infty \implies$ **FV effects parametrized in terms of infinite volume quantities**

Comparison of the FV corrections

Periodic boundary conditions (Hansen & Patella, 2019)

$$\Delta G^{1+3}(x_0|L) = -\frac{1}{3}\sum_{q=\pm1,0}\int\frac{dp_3}{2\pi}\frac{e^{-L\sqrt{m_\pi^2+p_3^2}}}{4\pi L}\times \mathrm{Re}\int\frac{dk_3}{2\pi}e^{ik_3x_0}\,T_q(-k_3^2,-k_3p_3)$$

- T_q forward Compton scattering amplitude
- dominant contribution from pion pole of $T_{\pm1} \propto F_\pi^2(-k_3^2)$ (space-like FF)

C* boundary conditions:

1. $\Delta G^{1,C^\star}(x_0|L) \to$ same contribution as with pbc, but only from T_0

2. $\Delta G^{2a+2b}(x_0|L) = \frac{2}{3}\int d^2\vec{x}_\perp \langle 0|\mathcal{J}_\mu(\underline{x})\frac{e^{-\frac{L}{2}H}}{H}\mathcal{J}^\mu(0)|0\rangle + (\underline{x}\leftrightarrow -\underline{x}) + O(e^{-\frac{3}{2}Lm_\pi})$

Comparison of the FV corrections

Periodic boundary conditions (Hansen & Patella, 2019)

$$\Delta G^{1+3}(x_0|L) = -\frac{1}{3}\sum_{q=\pm1,0}\int \frac{dp_3}{2\pi}\,\frac{e^{-L\sqrt{m_\pi^2+p_3^2}}}{4\pi L}\times \mathrm{Re}\int \frac{dk_3}{2\pi}\,e^{ik_3x_0}\,T_q(-k_3^2,-k_3p_3)$$

- T_q forward Compton scattering amplitude
- dominant contribution from pion pole of $T_{\pm1}\propto F_\pi^2(-k_3^2)$ (space-like FF)

C* boundary conditions:

1.$\Delta G^{1,C^\star}(x_0|L)\to$ same contribution as with pbc, but only from T_0

2.$\Delta G^{2a+2b}(x_0|L) = -\frac{1}{2\pi}\int dP_3\,e^{iP_3x_0}\int_{4m_\pi^2}^{\infty} ds\,\frac{e^{-\frac{L}{2}\sqrt{s+P_3^2}}}{s+P_3^2}\,s\rho_{\pi\pi}(s) + O(e^{-\frac{3}{2}Lm_\pi})$

- dominant contribution from $|F_\pi(s)|^2$ (time-like FF)

(Partial) Numerical estimates of FV effects with C*

1. Leading FV effects to HVP,LO at physical point: comparison pbc vs C* in 1D

- Leading FV corrections with C* bc

$$\Delta a_\mu^{\mathrm{HVP},1C^\star}(L) \simeq -\int_{4m_\pi^2}^{\infty} ds\, \mathcal{K}(s;L)\rho_{\pi\pi}(s)$$

- Omnès parametrization for $F_\pi(s)$

$$\exp\left(P_1(s)s + \frac{s^2}{\pi}\int_{4m_\pi^2}^{\infty} ds' \frac{\delta_1^{BW}(s)}{(s')^2(s'-s-i\epsilon)}\right)$$

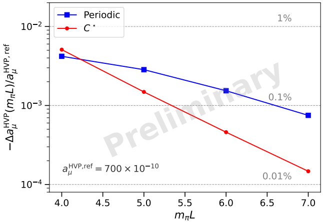

(Partial) Numerical estimates of FV effects with C*

1. Leading FV effects to HVP,LO at physical point: comparison pbc vs C* in 1D

- Leading FV corrections with C* bc

$$\Delta a_\mu^{\mathrm{HVP},1C^\star}(L) \simeq -\int_{4m_\pi^2}^{\infty} ds\, \mathcal{K}(s;L)\rho_{\pi\pi}(s)$$

- Omnès parametrization for $F_\pi(s)$

$$\exp\left(P_1(s)s + \frac{s^2}{\pi}\int_{4m_\pi^2}^{\infty} ds' \frac{\delta_1^{BW}(s)}{(s')^2(s'-s-i\epsilon)}\right)$$

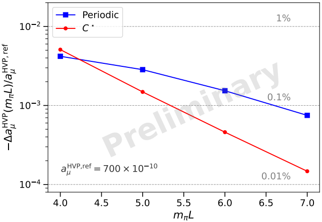

2. Estimates of FVE to $a_\mu^{33,\mathrm{IW}}$ with C* at larger m_π ($F_\pi(s)$ from Erben et al., 2019)

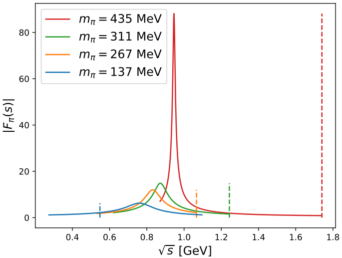

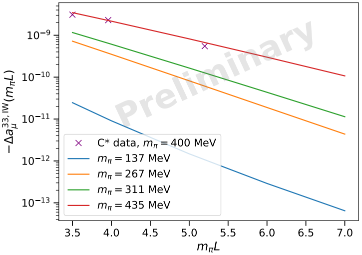

Conclusions

Summary & Outlook

1. Numerical study of L-dependence for $a_\mu^{33,\mathrm{IW}}$

   - Setup: 4 ensembles with $N_f = 3+1$, $m_\pi \simeq 400$ MeV, $m_\pi L \in [3.5, 7]$ and C* bc
   - Observed finite-L effects 2-3 times larger than estimates with pbc

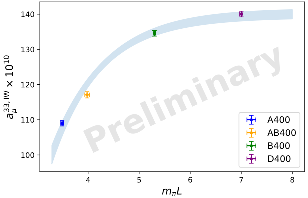

2. Analytical study of the leading spatial FV effects

   - Hamiltonian representation of the vector correlator (HP, 2019) applied to C*
   - Dominant contribution parametrized by the spectral density in the 2π region

$$G(x_0|L) - G(x_0|\infty) = -\int_{4m_\pi^2}^{\infty} ds\, \mathcal{K}(s; x_0, L)\rho_{\pi\pi}(s) + O(e^{-3m_\pi L/2})$$

$\implies$ enhanced FV effects at larger than physical m_π due to ρ resonance peak

Next steps:

- Obtain analytical expression beyond 1D case and the leading-order exponential
- Compare FV estimates with lattice results at close-to-physical pion mass
- Analytical and numerical study of FV effects to the HVP in full QCD+QED$_\mathrm{C}$

Thank you for your attention!

Backup

Motivation for C* boundary conditions

Charged states are forbidden in a finite periodic volume:

- Classical explanation $\rightarrow$ Gauss's law
- QFT explanation $\rightarrow$ zero-momentum mode of A_μ

Common prescriptions in finite volume are:

- $\mathrm{QED_L}$: impose the condition $\tilde{A}_\mu(k_0, \vec{0}) = 0 \ \forall k_0$ (Hayakawa and Uno arXiv:0804.2044)
- $\mathrm{QED_m}$: introduce regulator m_γ (Endres et al. arXiv:1507.08916)
- $\boxed{\mathrm{QED_C}\text{: use } C^\star \text{ (}C\text{-periodic) boundary conditions}}$ (Kronfeld and Wiese Nucl. Phys. B 357 (1991) 521,
- ...

$\mathrm{QED_C}$ preserves locality, gauge invariance and translation invariance

$$A_\mu(x + L_k\hat{k}) = -A_\mu(x) \qquad U_\mu(x + L_k\hat{k}) = U_\mu^*(x)$$

$$\psi(x + L_k\hat{k}) = C^{-1}\bar{\psi}(x)^\top \qquad \bar{\psi}(x + L_k\hat{k}) = -\psi^\top(x)\, C$$

$\star$ zero-momentum mode of A_μ absent by construction
$\star$ effective periodicity of $2L_k$ for all fields

Implementation of C* boundary conditions

$$A_\mu(x + L_k\hat{k}) = -A_\mu(x), \qquad U_\mu(x + L_k\hat{k}) = U_\mu^*(x),$$

$$\psi(x + L_k\hat{k}) = C^{-1}\,\bar{\psi}(x)^\top, \qquad \overline{\psi}(x + L_k\hat{k}) = -\psi^\top(x)\,C.$$

- Lattice is doubled in direction $\hat{1}$: $L_1 = 2L$, while $L_k = L$ for $k = 2, 3$.
- Orbifold construction: $\psi(x + L_k\hat{k}) = \psi(x + \frac{L_1}{2}\hat{1})$ for $k = 2, 3$

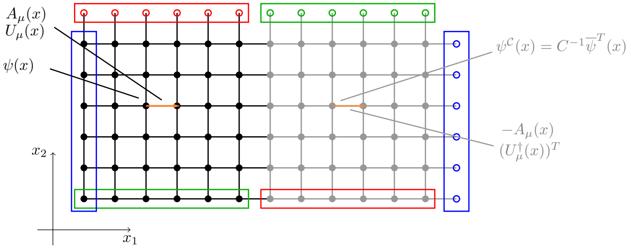

Implications of $C^\star$ boundaries - I

- Quark propagator in FV with periodic boundary conditions:

$$\left\langle \psi(x)\,\bar{\psi}(0) \right\rangle_L = \sum_{\vec{n}\in\mathbb{Z}^3} S(x - \vec{n}\cdot\vec{L})$$

- Quark propagators in FV with $C^\star$ boundary conditions (Lucini et al, 2015):

$$\left\langle \psi(x)\,\bar{\psi}(0) \right\rangle_L = \sum_{\{\vec{n}|\tilde{n}=0\}} S(x - \vec{n}\cdot\vec{L})$$

$$\left\langle \psi(x)\,\psi^\top(0) \right\rangle_L = -\sum_{\{\vec{n}|\tilde{n}=1\}} S(x - \vec{n}\cdot\vec{L})C^{-1}$$

$$\left\langle \bar{\psi}^\top(x)\,\bar{\psi}(0) \right\rangle_L = \sum_{\{\vec{n}'|\tilde{n}'=1\}} CS(x - \vec{n}'\cdot\vec{L})$$

Implications of $C^\star$ boundaries - II

Consider the bilinear $O = \bar{\psi}\Gamma\psi$ and the quark-connected part of $\langle O(x)O^\dagger(0)\rangle$

- Correlator with periodic boundaries:

$$\left\langle \bar{\psi}(x)\Gamma\psi(x)\bar{\psi}(0)\Gamma\psi(0) \right\rangle_L = -a^{-6}\,\mathrm{Tr}\left\{\Gamma D^{-1}(x|0)\Gamma D^{-1}(0|x)\right\}$$

- Correlator with $C^\star$ boundaries (implemented on the extended lattice):

$$\left\langle (\psi^\top TC)(x)\Gamma\psi(x)(\psi^\top TC)(0)\Gamma\psi(0) \right\rangle_L + \left\langle (\psi^\top TC)(x)\Gamma\psi(x)(\psi^\top TC)(0)\Gamma\psi(0) \right\rangle_L$$
$$= -a^{-6}\,\mathrm{Tr}\left\{\Gamma D^{-1}(x|0)\Gamma D^{-1}(0|x)\right\} \quad \underbrace{\pm a^{-6}\,\mathrm{Tr}\left\{\Gamma D^{-1}(x|L\hat{1})\Gamma D^{-1}(L\hat{1}|x)\right\}}_{\text{Additional contraction, sign depends on } C\text{-parity of } \Gamma}$$

Vector correlator: periodic vs C* boundary conditions

Periodic setup:

- $G(x + L\hat{3}) = G(x)$
- $G(x_0, x_\perp, -x_3) = G(x_0, x_\perp, x_3)$

$\implies G(x_0, x_\perp, L - x_3) = G(x_0, x_\perp, x_3)$

C* setup:

- $G(x + L\hat{3}) = -G(x)$
- $G(x_0, x_\perp, -x_3) = G(x_0, x_\perp, x_3)$

$\implies G(x_0, x_\perp, L - x_3) = -G(x_0, x_\perp, x_3)$

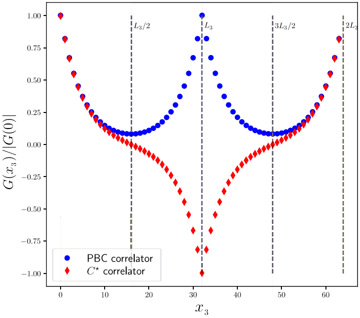

Integration domain irrelevant for pbc

With C* symmetric domain around source point

Discretization of $a_\mu^{33,\mathrm{lW}}$

Lattice estimators:

$$a_\mu^{33,\mathrm{l}} = \left(\frac{\alpha}{\pi}\right)^2 a \sum_{t=0}^{T/2} G^{33,\ell}(t) \tilde{K}(t; m_\mu) w_\mathrm{l}(t), \qquad \ell = \mathrm{l,c}$$

where $G^{33,\ell}$ is

$$G^{33,\mathrm{l}}(t) = (Z_\mathrm{V}^\mathrm{m})^2 G_\mathrm{bare}^{33,\mathrm{l}}(t), \qquad G^{33,\mathrm{c}}(t) = Z_\mathrm{V}^\mathrm{m} G_\mathrm{bare}^{33,\mathrm{c}}(t).$$

- $\ell = l \to$ local-local discretization
- $\ell = c \to$ point-split local discretization

$$\tilde{V}_\mu(x) = \bar{\psi}(x + a\hat{\mu}) \frac{1+\gamma_\mu}{2} U_\mu^\dagger(x + a\hat{\mu}) \psi(x) - \bar{\psi}(x) \frac{1-\gamma_\mu}{2} U_\mu(x) \psi(x + a\hat{\mu})$$

Renormalization condition: (mass-dependent scheme):

$$\lim_{t\to\infty} \frac{Z_\mathrm{V}^\mathrm{m} G_\mathrm{bare}^{33,\mathrm{l}}(t)}{G_\mathrm{bare}^{33,\mathrm{c}}(t)} = 1.$$

Dominant contributions to FV effects with C* bc

Leading contributions to $\Delta G^{2a}(x_0|L)$

- $|\Psi^3\rangle = \frac{\varepsilon^{3bc}}{\sqrt{2}}|\pi^b(\vec{p})\pi^c(\vec{p}')\rangle \to |\langle 0|\mathcal{J}^3_\mu|\Psi^3\rangle|^2 = 2(p-p')^2_\mu |F_\pi(s)|^2$

Pair production

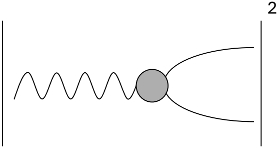

$$\Delta G^{2a}_{\pi\pi}(x_0|L) = -\frac{1}{\pi}\int dP_3 \cos(P_3 x_0)\int_{4m_\pi^2}^{\infty} ds\, e^{-\frac{L}{2}\sqrt{s+P_3^2}}\,\frac{s}{s+P_3^2}\underbrace{\frac{|F_\pi(s)|^2}{48\pi^2}\left(1-\frac{4m_\pi^2}{s}\right)^{3/2}}_{\rho_{\pi\pi}(s)}$$

- $\langle 0|\mathcal{J}^8_\mu|\pi\pi\pi, I=0, C=-1, P=-1\rangle \to\ O(e^{-3Lm_\pi/2})$ contribution

Integrand $K(s)\rho(s)$ at the physical m_π

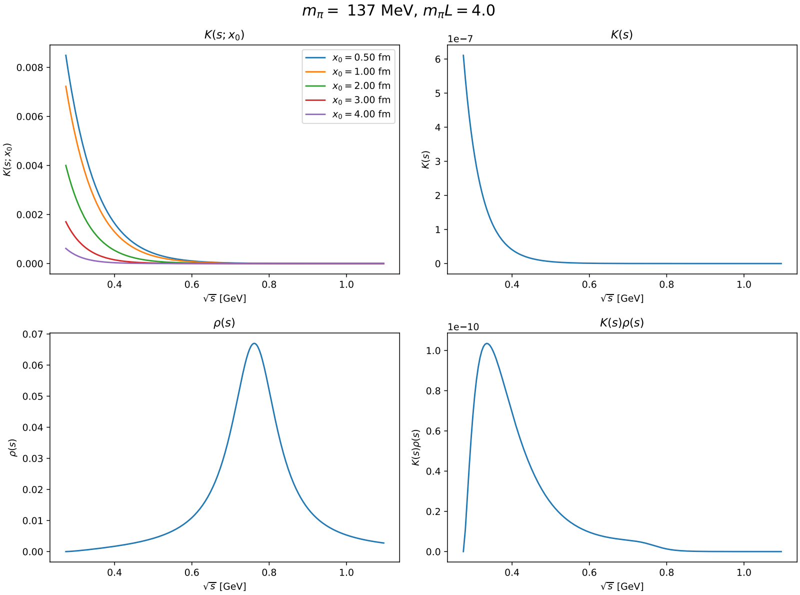

Integrand $K(s)\rho(s)$ at unphysical m_π-I

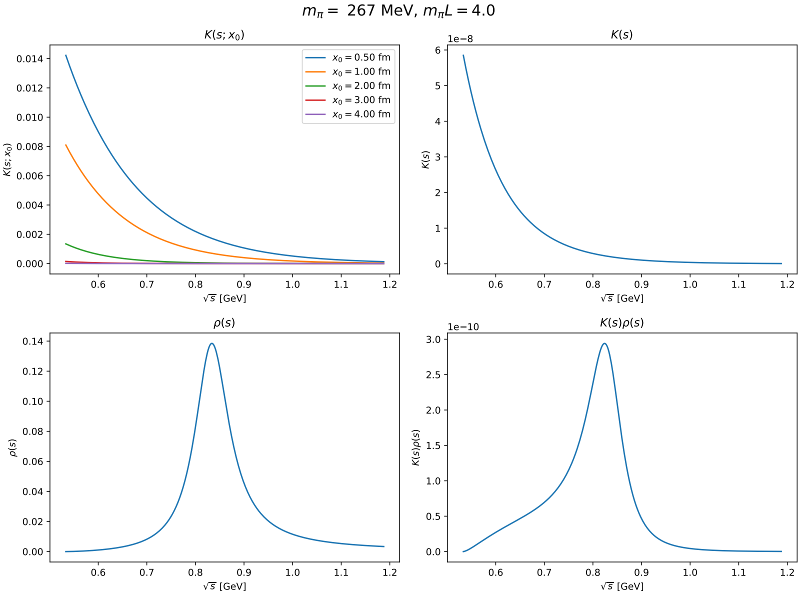

Integrand $K(s)\rho(s)$ at unphysical m_π-II

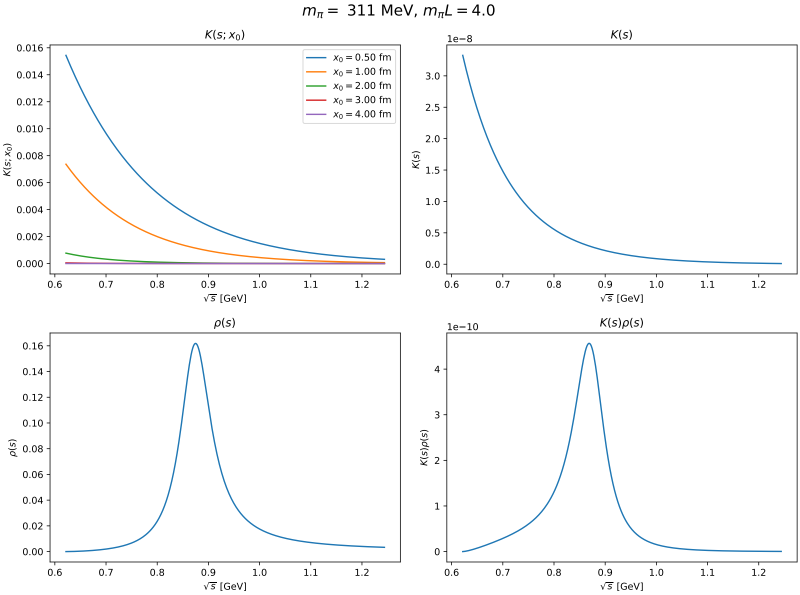

Integrand $K(s)\rho(s)$ at unphysical m_π-III